13th International Conference on Applications of Statistics and Probability in Civil Engineering, ICASP13
Seoul, South Korea, May 26-30, 2019

Performance of Nonstructural Components in NPPs under High-Frequency Ground Motions

Jieun Hur
Visiting Assistant Professor, Dept. of Civil, Environment and Geodetic Engineering, The Ohio State University, Columbus, OH, U.S.A.

Abdollah Shafieezadeh
Associate Professor, Dept. of Civil, Environment and Geodetic Engineering, The Ohio State University, Columbus, OH, U.S.A.

ABSTRACT: This study evaluates the seismic performance of nonstructural components subjected to strong high frequency ground motions (GMs), and further investigates the acceleration amplification factors considering involved uncertainties. For this purpose, a set of ground motion histories are modified to match the ground motion response spectrums for NPP sites in the western and eastern U.S. The seismic performance of nonstructural components is analyzed through time history analysis. Using this procedure, acceleration responses of floors and nonstructural components are evaluated, and the variation of amplification factors are estimated. For nonstructural components attached to structures with high natural frequency, the amplification factors can be large under GMs with high frequency contents compared to GMs with normal frequency contents. However, this may not lead to increased failure probabilities under GMs with high frequency contents.

1. INTORDUCTION

Some nonstructural components (NSCs) such as electrical equipment have critical roles in the proper functionality of nuclear power plants (NPPs). Most of these components with relay or other control switches are categorized as acceleration sensitive, and can be vulnerable to ground motions with high frequency content. EPRI technical report (EPRI, 2007) also described that a significant amount of empirical and theoretical evidence, as well as regulatory precedents, support the conclusion that high-frequency vibratory motions above about 10 Hz are not damping to the large majority of NPP structures, components, and equipment (Richards et al., 2015)

Meanwhile, recent strong earthquakes have prompted the need for more studies about the seismic damage to NSCs including their operational failures. Although there was no safety related damage to nuclear power plants during Virginia Earthquake in 2011, the ground motions at a plant site exceeded a portion of the seismic design basis. The Great Tohoku Earthquake in 2011, which is one of the largest earthquakes in recorded history, caused operational failures in several nuclear power plants. Following these accidents, the nuclear regulatory commission (NRC) has examined the seismic safety of NPPs in the US and recently has stated that a risk-informed performance-based ground motion response spectrum (GMRS) can exceed the safe-shutdown earthquake (SSE) in high frequency range (EPRI, 2015). Based on the updated GMRS, NPP sites in the central and eastern United State (CEUS) contain more high-frequency contents in the ground motions as shown in Figure 1. The EPRI report suggests the modification of amplification factors for nonstructural components depending on the level of the floor where the nonstructural components are attached (EPRI, 2015).

Nuclear structures (existing plants and new designs) are very stiff with fundamental frequencies in the range of 3-15 Hz. In structural engineering, building structures with fundamental frequencies greater than 4 Hz are often regarded as high frequency structures, while nuclear plant structures with fundamental frequencies greater than 10 Hz are considered as high frequency structures. In general, most nuclear structures have fundamental frequencies less than 10 Hz in the horizontal directions and would not be expected to have significant horizontal response to site-specific spectral models that have high accelerations in the frequency range above 10 Hz. (EPRI , 2015)

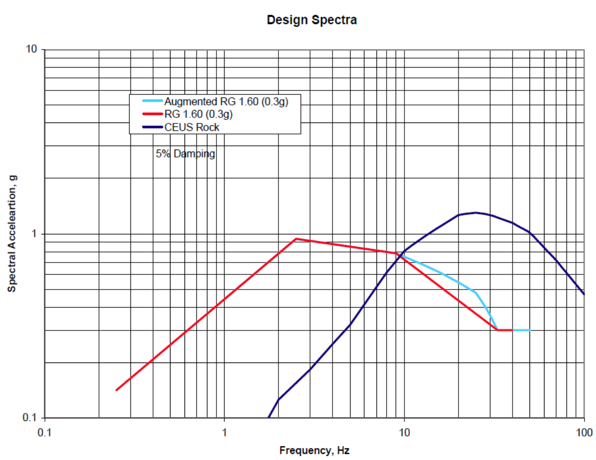

Figure 1: Comparison of a Design Motion Developed for a CEUS Rock Site and Design Motions Used for Design Certification (5% Damping) (EPRI, 2015)

However, this guidance has been developed based on the limited studies regarding the impacts of high frequency contents of ground motions on NSCs in NPPs. This study evaluates the amplification factors for the acceleration response of nonstructural components attached to an auxiliary building with respect to peak ground acceleration and peak floor accelerations. To quantify the impact of high frequency contents of ground motions on NSCs, a set of ground motion histories is selected and modified to match the GMRS for an auxiliary building of a hypothetical NPP for two locations in south eastern and western US. The seismic performance of nonstructural components is estimated using time history analysis considering the dynamic behavior of the building. Using this procedure, acceleration and displacement responses of NSCs are evaluated, and the amplification factors and failure probabilities of NSCs are estimated considering involved uncertainties for each set of ground motions.

2. MODEL DESCRIPTION

2.1. Selection of Ground Motion Histories

In order to evaluate the impact of the ground motions with high frequency contents, two sets of ground motion histories are generated to represent two locations in the CEUS region (Savannah, GA) with high frequency contents and California region (Long beach) with relatively low frequency contents as shown in Figures 2 and 3. First, 18 ground motions are selected from the PEER ground motion database. They follow the strike-slip fault mechanism, and it is assumed that their mean shear-wave velocity over the top 30 m (Vs30) is at least 800 m/sec. Their time steps are modified so that the dominant periods of the pseudo-acceleration response spectra are relatively close to that of the target spectrum of each location, and the durations of the ground motions are acceptable. Finally, the motion records with modified time steps are matched to the target spectrum using the SeismoMatch software (SeismoSoft, 2010), which also conducts baseline correction. This program uses the wavelets algorithm proposed by Abrahamson (1992) and Hancock et al. (2006), which are based on the time-domain method developed by Lilan and Tseng (1988) with some modifications to conserve non-stationarity at long periods. In Figures 2 and 3, the red dashed lines show the mean values of the spectral acceleration for 18 ground motions. For the mean responses, peak spectrum accelerations (PSa) are 0.815 g and 0.822 g for high frequency and low frequency ground motions, respectively. Their peak ground accelerations (PGA) are also very close to each other. The mean PGA of 18 sets of ground motions with high frequency contents is 0.321 g, and that of GMs with normal frequency contents is 0.333 g.

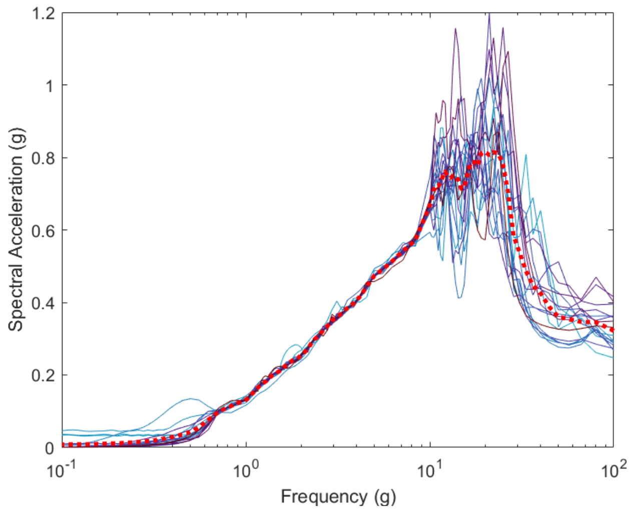

Figure 2: Spectral Accelerations of 18 sets of ground motions in the CEUS (Damping 5%)

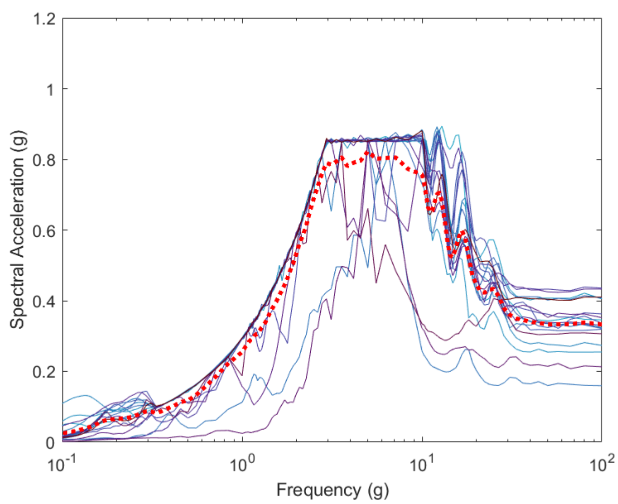

Figure 3: Spectral Accelerations of 30 sets of ground motions in the Western (Damping 5%)

2.2. Model Descriptions of NSCs in an Auxiliary Building in NPPs

In order to evaluate the acceleration response of NSCs, it is assumed that NSC1 and NSC2 represent essential electrical equipment in an auxiliary building of a nuclear power plant, and they are mounted on each floor of a two-story auxiliary building as shown in Figure 4. It is assumed that two identical auxiliary buildings are located in western and eastern U.S. Figure 4 illustrates: (a) the simplified model of the two-story auxiliary building in a pseudo-plant, (b) a stick model used for the characterization of the building with non-structural components NSC1 and NSC2 affixed to the first and second floors of the building, and (c) the nonstructural components restrained on floors. In this study, the auxiliary building is assumed to be stiff and have a high fundamental frequency of 12.5 Hz, which is chosen since the nuclear structures are stiff and their fundamental frequencies are in the range of 3~15 Hz (EPRI, 2015).

For the building structure, a lumped-mass stick model is used and a set of ground motion histories is applied in the horizontal direction. From the analysis, the seismic response of a component is evaluated and compared to corresponding limit-states to estimate the failure probability of the equipment.

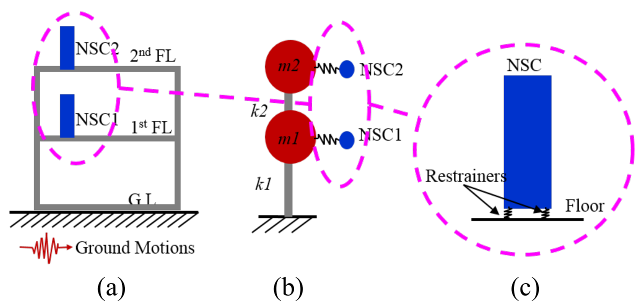

Figure 4: Simplified Models for a Building in a NPP

According to the literature review on the fragility functions of electrical equipment based on shaking table tests (Ellingwood, 1998; NUREG, 1987), the capacity function of a specific type of DC battery rack is assumed as a lognormal distribution with a median failure value of 1.01 g with β_R = 0.28, and β_U = 0.63. It assumed that one type of electrical equipment is used for different levels and their capacity are identical. The limit state function is randomly generated based on the lognormal distribution of the DC batter rack as shown in Table 1.

Based on the assumption that the mean value of the fundamental frequency of the building is 12.5 Hz, the mass (m1 and m2) and stiffness (k1 and k2) of the two floors of the structure are sampled as shown in Table 1. Due to potential variation in the dimensions of structural components and uncertainty in their material properties, it is assumed that the distribution of mass and stiffness is normal with 10% coefficient of variation for each variable, which includes the construction and structural analysis errors in reinforced concrete buildings. The damping effect of the building structure is also considered with a damping ratio (ζ_B). It is assumed that ζ_B is uniformly distributed between 2% and 5%. These values are typical damping ratios for reinforced concrete and steel structures in practice (IBC, 2006).

The dynamic response of a nonstructural component, specifically the battery rack, depends on the location of the component in the building and the types of restraints. In this study, it is assumed that the battery racks are fastened or fixed to each floor. The seismic response of these components is computed based on the seismic response of the corresponding floor of the building and the fundamental frequency (T_{NSC}) of the battery rack when treated as a single degree of freedom (SDOF) as shown in Fig. 1(b). Most types of electrical equipment in nuclear power plants are required to pass a certain level of shaking table tests for their seismic qualification. One type of such tests is the resonance test. These tests show that the fundamental frequency of most electrical equipment is in the range of 4-16 Hz (Hur, 2012; Kim et al., 2012). Thus, this study assumes that the fundamental frequencies of the battery racks follow a uniform distribution from 4 to 16 Hz. These frequencies can be lower, if battery racks are not fully restrained (Hur, 2012).

2.3. Parameters for Sampling

Several properties of the structural system are considered as random variables to account for uncertainties in the simulations. They include the mass of the building floors m1 and m2, stiffness of each story k1 and k2, damping of the building ζ_B, fundamental frequency of nonstructural components (T_{NSC}), and the operational capacity of nonstructural components. In order to reduce the number of simulations, the mass and lateral stiffness of two stories are considered identical (m1 = m2 and k1 = k2). Therefore, total five variables are considered. Their distributions are summarized in Table 1. The table shows each variable and its unit and distributions. Here, N, U and L denote the normal, uniform, and lognormal distribution, respectively, and C.O.V. represents the coefficient of variation. Based on the 1,000 samples of m1=m2 and k1=k2, the fundamental frequency of building (F_B) follows a normal distribution with mean of 12.5 Hz and coefficient of variation of 7.3%. The fundamental frequency of NSC (F_{NSC}) is 4-16 Hz, and it means that the natural period of NSC is 0.006 to 0.25 seconds. The operational capacity of NSC is assumed to follow a lognormal distribution, and therefore, Exp(μ) is the mean value and Exp(μ + σ) is the variation of the normal distribution.

Table 1: Variable Parameters

		Mean	C.O.V.	Dist.*
m1 = m2	(kN*s^2/m)	25	0.1	N
k1 = k2	(kN/m)	40E+4	0.1	N
F_B	(Hz)	12.5	0.073	N
		Min	Max	Dist.*
ζ_B	(ratio)	0.02	0.05	U
F_{NSC} T_{NSC}	(Hz) (sec)	4 0.006	16 0.25	U
		μ	σ	Dist.*
Capacity	(g)	1.01	0.063	L

*: Dist.=Distribution; N=Normal; U=Uniform; L= Lognormal

This study focuses on the evaluation of acceleration amplification factors of NSCs under two sets of GM histories. To consider effects of uncertainties, 1,000 samples are generated using Latin Hypercube Sampling (LHS) technique.

3. DYNAMIC ANALYSIS

Using the ground motion histories, two sets of time history analyses are conducted for the same sample. For the MC simulations, each input variable set from 1,000 samples goes to the dynamic analysis in order to obtain the dynamic response of two floors at the locations of the equipment as well as the absolute accelerations of the equipment by solving the following equation:

$$M\begin{Bmatrix}\ddot{u_1}\\ \ddot{u_2}\end{Bmatrix} + C\begin{Bmatrix}\dot{u_1}\\ \dot{u_2}\end{Bmatrix} + K\begin{Bmatrix}u_1\\ u_2\end{Bmatrix} = -Ml\ddot{u}_g \qquad (1)$$

where $M = \begin{bmatrix} m1 & 0 \\ 0 & m2 \end{bmatrix}$ is the mass matrix, $K = \begin{bmatrix} k1+k2 & -k2 \\ -k2 & k2 \end{bmatrix}$ is the stiffness matrix, $C = a_0M + a_0K$ is the damping matrix with $a_0 = \frac{2\zeta\omega_1\omega_2}{\omega_1+\omega_2}$ and $a_1 = \frac{2\zeta}{\omega_1+\omega_2}$.

Equation (2) is solved using the Bogachi-Shampine method (MATLAB, 2012) which is implemented in the function, ode 23, in MATLAB (MATLAB, 2012). It is a Runge–Kutta method of order three with four stages with the First Same As Last (FSAL) property, so that it uses approximately three function evaluations per time step. The solution of Eq. (1) provides: (1) the absolute floor accelerations FA1 ($\ddot{u_1}$) and FA2 ($\ddot{u_2}$), and (2) floor displacemens FD1 (u_1) and FD2 (u_2). Using these histories of FA1 and FA2, fundamental frequencies of non-structural components (NSCs), T_{NSC}, and a constant damping ratio of 5% for the NSC, acceleration response histories of NSCs are computed.

4. ANALYSIS RESULTS

The same 1,000 sample set goes to the dynamic anlaysis under each set of ground motions.

4.1. Dynamic Analysis Results for GM Sets with High-Frequency Contents

Figure 5 illustrates the peak acceleration (PA) responses of NSCs with respect to model parameters. In the vast majority of cases, the acceleration response of NSC2 located on the second floor is larger than the acceleration of NSC1, which is located on the first floor.

Depending on values of mass, stiffness, and fundamental frequencies of a building, the acceleration response of NSC1 and NSC2 are normally distributed. Damping ratios rarely impact the acceleration response of NSCs. As shown in Figure 4(e), the acceleration response of NSCs around the fundamental frequency of the NSCs of 12.5 Hz is very high. This is because of the fact that this frequency coincides with the fundamental frequency of the building thus leading to resonance effects.

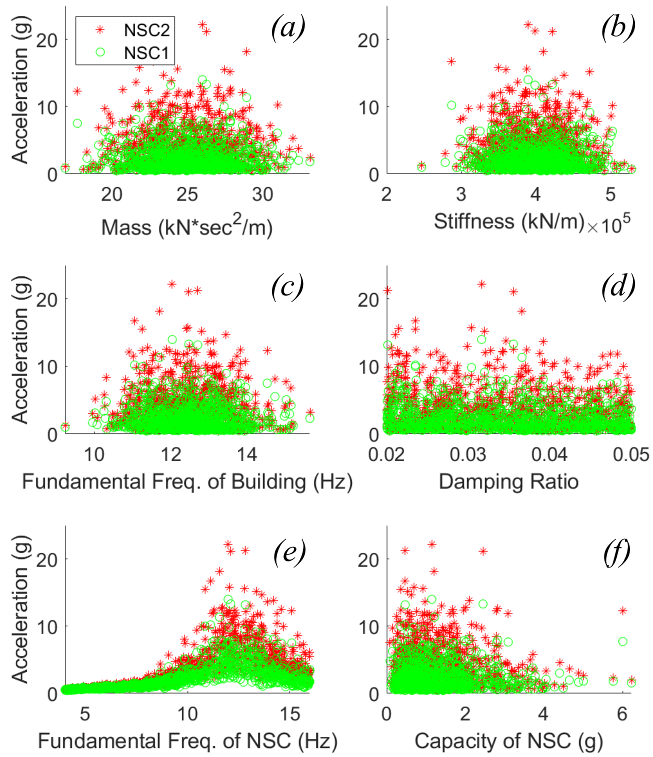

Figure 5: Analysis Result of Samples under GMs with High Frequency Contents for CEUS region

Figure 6 shows the distribution of the response acceleration of NSCs from the 1,000 sample. This distribution is close to the lognormal distribution.

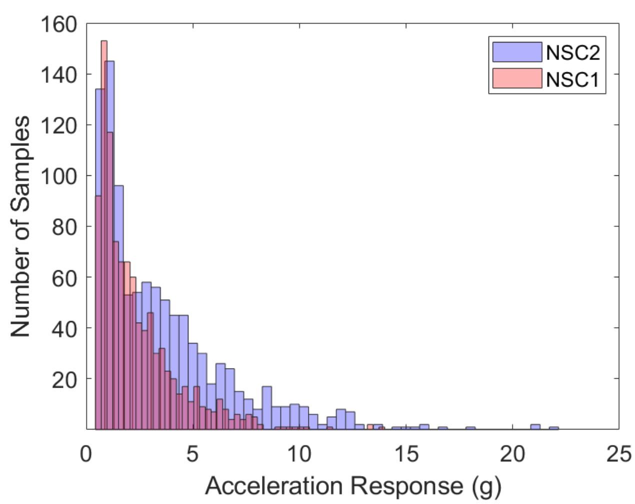

Figure 6: Histogram of Acceleration Response of NSCs under GMs with High Frequency Contents for CEUS region

4.2. Dynamic Analysis Result for GM sets with Low-Frequency contents

Figure 7 illustrates the peak acceleration (PA) responses of NSCs with respect to model parameters under the ground motions with normal frequency contents. It can be compared to Figure 5 that illustrates the PA responses of NSCs under GMs with high frequency contents. Since the same sets of samples are used for Figures 5 and 7, the distributions of model parameters are the same, and the trends of distributions are simliar. However, the maximum PA responses of NSCs under GMs with high frequency contents in Figure 5 are higher than those in Figure 7.

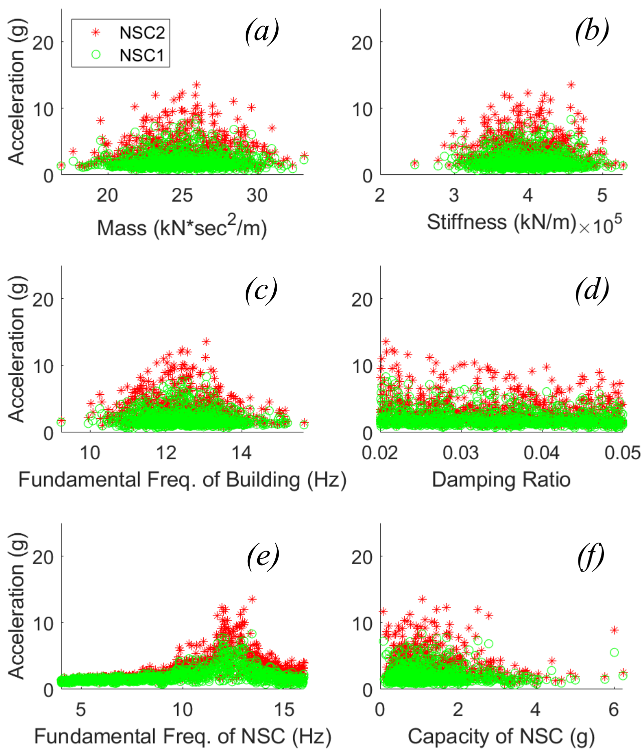

Figure 7: Analysis Result of Samples under GMs with Normal Frequency Contents for California region

Figure 8 shows the distribution of the response acceleration of NSCs from the 1,000 sample, which are under GMs with normal frequency contents. It is also close to the lognormal distribution, similar to the case in Figure 6. However, the distribution of PA responses in Figure 8 is narrow compared to those in Figure 6 indicating that the dispersion of PA responses of NSCs under GMs with normal frequency contents is much smaller.

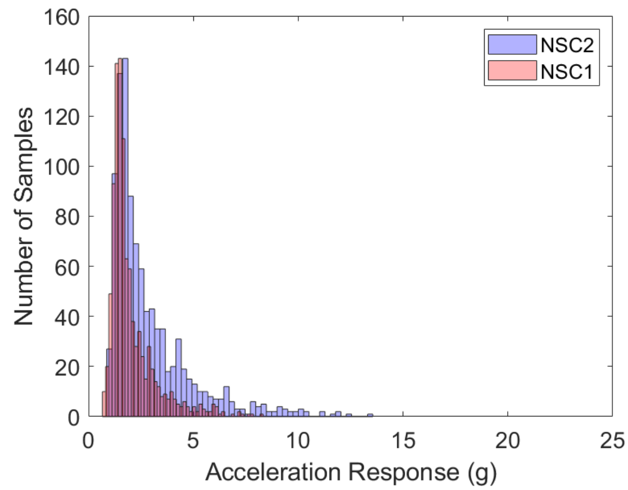

Figure 8: Histogram of Acceleration Response of NSCs under GMs with Normal Frequency Contents for California region

4.3. Amplification Factors for NSCs

Based on the analysis results, the acceleration amplification factors (AFs) for the NSCs are estimated with respect to the PGA and Peak Floor Accelerations (PFA), respectively. PFA_1 and PFA_2 indicate the peak floor acceleration of the first and second floor, respectively. These distributions are fitted to each lognormal distribution, and its parameters are summarized in Table 2 and Figures 9 (a) and (b).

Table 2: Amplification Factors (Lognormal Dist.)

High Frequency	μ	σ
PAs of NSC1 / PFA_1	1.0975	0.7264
PAs of NSC2 / PFA_2	0. 9451	0. 8602
PAs of NSC1 / PGA	1.7647	0.7409
PAs of NSC2 / PGA	2.1068	0.8738
Low Frequency	**μ**	**σ**
PAs of NSC1 / PFA_1	1.5515	0.4387
PAs of NSC2 / PFA_2	1.3587	0.5327
PAs of NSC1 / PGA	1.6777	0.4910
PAs of NSC2 / PGA	1.9674	0.5965

As shown in Table 2, the dispersion of PA responses of NSCs under GMs with high frequency contents are much higher than those under GMs with normal frequency contents. As expected, the AFs with respect to PFAs are smaller than AFs with respect to PGAs. The AFs w.r.t. PGAs of NSCs under GMs with high frequency contents are higher than those under GMs with normal frequency contents. However, the AFs w.r.t. each PFA of NSCs under GMs with high frequency contents are smaller than those under GMs with normal frequency contents.

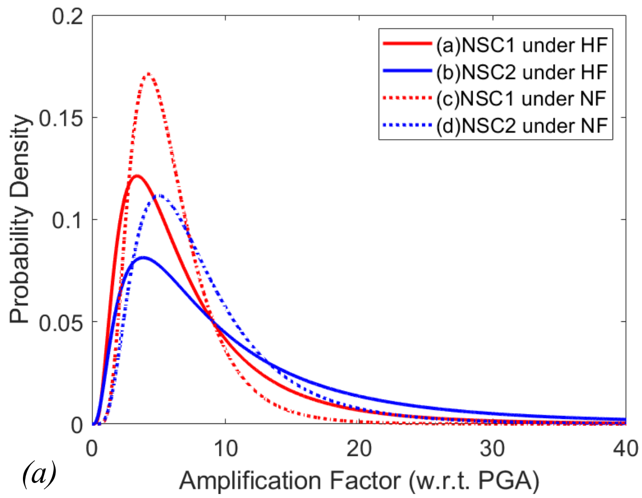

(a)

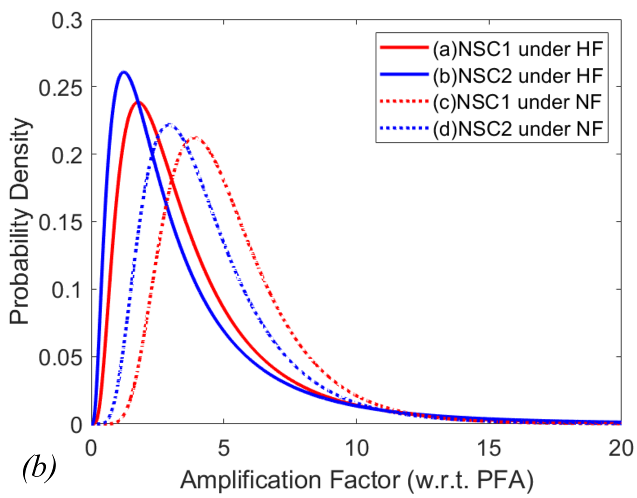

(b)

Figure 9: Probability Density Functions of Amplification Factors for NSCs (Note that HF: GMs in CEUS region with high frequency contents; NF: GMs in California region with normal frequency contents)

Figures 9 (a) and (b) illustrate the probabilistic density functions of AFs with respect to PGAs and PFAs, respectively. As shown in Figure 9 (a), the AFs of NSC2 are higher than those of NSC1 for both GM sets, and their dispersions are also larger than those of NSC1. Even though NSCs for all cases are identical, AFs w.r.t. PFAs are different as illustrated in Figure 9 (b), and those of NSC2 are smaller than those of NSC1 for both GM sets. The dispersion of AFs w.r.t. PFAs are much smaller than those w.r.t. PGAs.

4.4. Failure Probability of NSCs

Failure probabilities of identical NSCs mounted on identical buildings in two locations subjected to different seismic shakings are estimated, and their values are summarized in Table 3. Since this analysis used a low threshold for the capacity of the NSC, the failure probabilities are relatively high, and the failure probabilities of NSCs under GMs with normal frequency contents are higher.

Table 3. Failure Probabilities of NSCs

GMs with	NSC1	NSC2
High frequency contents (for CEUS region)	0.70	0.78
Normal frequency contents (for California region)	0.77	0.84

5. CONCLUSIONS

This study investigated the acceleration amplification factors of nonstructural components (NSCs) mounted on floors of a building to evaluate the impact of ground motions (GMs) with high frequency contents. For this analysis, two sets of GMs are generated for two different locations to represent eastern and western U.S. LHS technique did enable the uncertainty assessment considering various random variables.

Results of this study will enhance the understanding of the seismic safety of nonstructural components under strong high frequency ground motions. It will also facilitate seismic probabilistic risk assessments (SPRAs) of NPPs by quantifying the probabilistic safety of nonstructural components in NPPs.

6. REFERENCES

Abrahamson N.A. (1992), "Non-stationary spectral matching," *Seismological Research Letters*, Vol. 63, No. 1, p. 30.

Electric Power Research Institute (2007), "Program on Technology Innovation: Seismic Screening of Components Sensitive to High-Frequency Vibratory Motions," *EPRI 1015109*, Palo Alto, CA, October.

Electric Power Research Institute (2015), "High Frequency Program: Application Guidance for Functional Confirmation and Fragility Evaluation," *EPRI Report 3002004396*, ADAMS Accession Number ML 15223A102.

Ellingwood, B. R. (1998) , "Issues related to structural aging in probabilistic risk assessment of nuclear power plants," *Reliability Engineering & System Safety62.3*: 171-183.

Hancock, J., Watson-Lamprey, J., Abrahamson, N.A., Bommer, J.J., Markatis, A., McCoy, E., Mendis, R. (2006) , "An improved method of matching response spectra of recorded earthquake ground motion using wavelets." *Journal of Earthquake Engineering*, Vol. 10 pp. 67–89.

Hur, J., Guler, A., Sezen, H., Aldemir, T., & Denning, R. (2016), "Assessment of conservatism in the separation of variables approach to seismic probabilistic risk assessment", Proceedings of *The International Congress on Advances in Nuclear Power Plants (ICAPP)*, San Francisco, CA, April 17-20, 2016.

Hur, J. (2012) , "Seismic performance evaluation of switch-board cabinets using nonlinear numerical models," *Georgia Institute of Technology*, Atlanta, GA.

IBC, ICC. (2006) "International building code," *International Code Council, Inc.*(formerly BOCA, ICBO and SBCCI) 4051: 60478-5795.

Kim, M. K., Choi, I. K. and Seo, J. M. (2012), "A shaking table test for an evaluation of seismic behavior of 480V MCC", *Nuclear Engineering and Design,* 243: 341-355 (2012)

Lilhanand, K., Tseng, W.S. (1988), "Development and application of realistic earthquake time histories compatible with multiple-damping design spectra," *Proceedings of the 9th World Conference on Earthquake Engineering,* Tokyo, Japan, Vol II, 819-824.

Mathworks, (2012) , "Bioinformatics Toolbox: User's Guide," The MathWorks, Inc. R2012a

Richards, J., Merz, K., & Hardy, G., (2015), "High Frequency Seismic Testing Of Potentially Sensitivity Components," *Proceedings of SMiRT-23*, Manchester, United Kingdom, August 10-14, 2015.

Shampine, L.F. and Reichelt, M.W. (1997) , "The Matlab ODE Suite,", *SIAM Journal on Scientific Computing* 18 (1): 1–22.

Seismosoft (2013), "Seismomatch v2.1 A computer program for spectrum matching of earthquake records," SeismoSoft.